Synthesis of Silicon Carbide Nanostructures via a Simplified Yajima Process—Reaction at the Vapor–Liquid Interface**

By *Chia-Hsin Wang*, *Yu-Hsu Chang*, *Ming-Yu Yen*, *Chih-Wei Peng*, *Chi-Young Lee*, and *Hsin-Tien Chiu**

Silicon carbide is a wide-bandgap semiconductor with many potential high-technology applications.[1,2] There are several ways to prepare silicon carbide powders and thin films. These include carbothermic reduction of silica, sol–gel synthesis, and various chemical vapor deposition techniques.[3–9] In 1975, Yajima reported a preceramic polymer route to prepare β-SiC fibers industrially.[10–14] In this process, Na was employed to couple $SiMe_2Cl_2$ monomers in hydrocarbon solvents into poly(dimethylsilane), $-(Me_2Si)_n-$. The preceramic polymer $-(Me_2Si)_n-$ was further thermally decomposed into the β-SiC fibers. Now, we wish to demonstrate that the original Yajima process can be simplified to generate β-SiC nanostructures efficiently. Cubic cages, cubic shells, and nanoparticles of β-SiC are formed via the reactions involving liquid Na and the vapors of the methylchlorosilanes $SiMe_2Cl_2$ and $SiMeCl_3$.

At 623 K and under 1 atm of Ar (1 atm = 101.325 kPa), NaH powders were decomposed to form small droplets of liquid Na. Then, the liquid Na was reacted with $SiMe_2Cl_2$ or $SiMeCl_3$ vapors to generate particle precursors **Pre-I** and **Pre-II**, respectively.

(The characterization of **Pre-I** and **Pre-II** is discussed below). After the precursors were decomposed at 1273 K under vacuum, fine powders were collected as the final products. Black powder **I** and yellow powder **II** were obtained from **Pre-I** and **Pre-II**, respectively.

As shown by the scanning electron microscopy (SEM) images in Figure 1, the particles of **I** display two types of morphologies. Particles possessing the major type, **Ia**, are hollow cubic cages with edge lengths of 60–400 nm (Fig. 1A). Many of the cages show edge thicknesses of ca. 40 nm. Energy dispersive spectroscopy (EDS) analysis suggested that **Ia** contains Si, C, and some O. Particles possessing the minor morphology type, **Ib**, are cubes with an edge length of 1–2 μm, as shown in Figure 1B. The EDS spectrum of **Ib** suggests that the cages are also composed of Si, C, and a small amount of O. Transmission electron microscopy (TEM) images of **Ia** and **Ib** are shown in Figures 1C,D, respectively. The TEM image of **Ia** confirms that the inner space defined by the cage's edges is empty. The electron diffraction (ED) study of **Ia** shows a diffused-ring pattern, indicating that the structure is polycrystalline. The ED rings can be indexed to the (111), (220), and (311) planes of a cubic structure. The lattice parameter a is estimated to be 0.435 nm, close to the value of β-SiC.[15] The TEM image in Figure 1D shows that **Ib** is composed of hollow cubes with wall thicknesses of ca. 20 nm. The ED pattern and the derived lattice parameter, $a = 0.435$ nm, suggest that **Ib** is also polycrystalline β-SiC.[15] Furthermore, X-ray diffraction (XRD) and other spectroscopic data, such as Fourier-transform infrared (FTIR) spectroscopy, ^{29}Si solid-state nuclear magnetic resonance (^{29}Si SSNMR), and X-ray photoelectron spectroscopy (XPS), support that **I** is mainly composed of β-SiC.

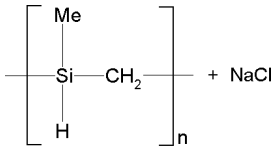

Pre-I

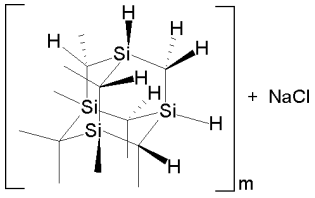

Pre-II

By employing $SiMeCl_3$ in the reaction, **Pre-II** was generated at 623 K. Unlike **Pre-I**, which showed significant weight loss above 873 K (40 % at 1023 K) in a thermogravimetric analysis (TGA), **Pre-II** was more stable up to 1023 K (8 % weight loss at 1023 K). After the precursor **Pre-II** was decomposed at 1273 K, **II** was isolated. An SEM image (Fig. 2A) shows the morphology of **II**, which consists of spherical nanoparticles with diameters of ca. 10 nm. The EDS result shows the presence of Si and C atoms. A TEM image (Fig. 2B) confirms that **II** has a nearly non-agglomerated spherical shape, with an average diameter of 10 nm. An ED study (Fig. 2C) shows a ring pattern that can be assigned to the diffractions from the (111), (200), (220), and (311) planes of cubic-phase polycrystals. From the ED, the lattice parameter a is estimated to be 0.435 nm. This is consistent with the literature value for

[*] Prof. H.-T. Chiu, C.-H. Wang, Dr. Y.-H. Chang, C.-W. Peng
Department of Applied Chemistry
National Chiao Tung University
Hsinchu 30050 (Taiwan)
E-mail: htchiu@cc.nctu.edu.tw
Dr. M.-Y. Yen
Materials Research Laboratories
Industrial Technology Research Institute
Hsinchu 31040 (Taiwan)
C.-W. Peng
Laboratoire de Physique Cristalline
Institut des Matériaux Jean Rouxe
2 rue de la Houssinière, BP 32229
F-44322 Nantes Cedex 3 (France)
Prof. C.-Y. Lee
Materials Science Center
National Tsing Hua University
Hsinchu 30043 (Taiwan)

[**] This work was supported by NSC92-2113-M-009-022 of the National Science Council of the Republic of China.

 DOI: 10.1002/adma.200400939

ADVANCED MATERIALS

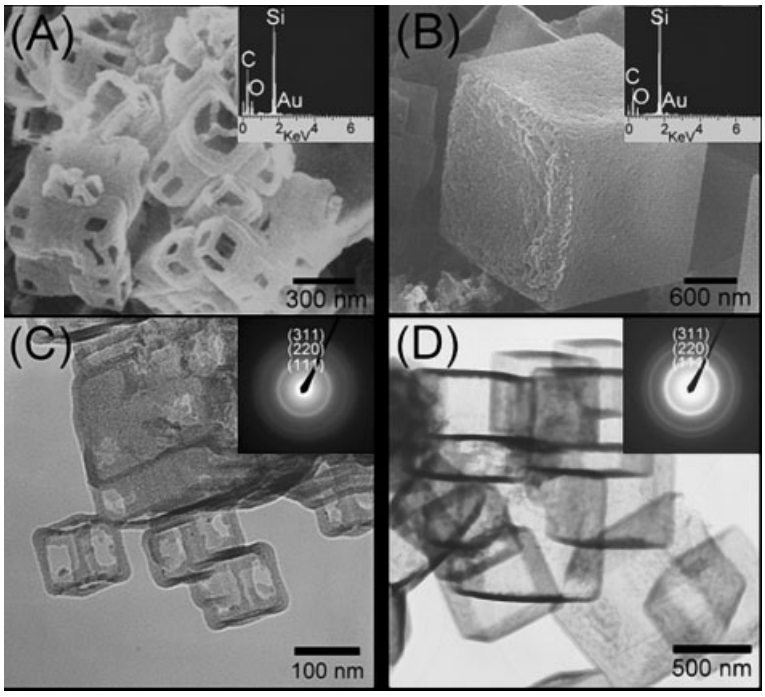

Figure 1. Images of **I**, prepared from $SiMe_2Cl_2$ and Na. SEM images and energy dispersive spectroscopy (EDS) spectrum (insets) of A) **Ia**; B) **Ib**. Transmission electron microscopy (TEM) images and electron diffraction (ED) patterns (insets) of C) **Ia**; D) **Ib**.

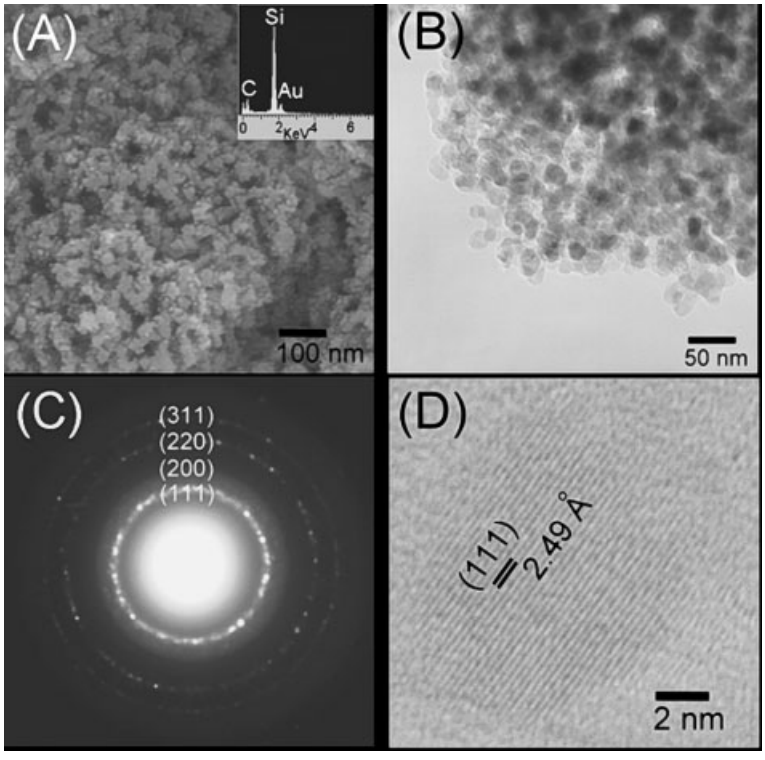

Figure 2. Images of **II**, prepared from $SiMeCl_3$ and Na. A) SEM image and EDS spectrum (inset); B) TEM image; C) ED pattern; D) high-resolution TEM image.

β-SiC.[15] A high-resolution TEM (HRTEM) image of a nanoparticle of **II** is shown in Figure 2D. The particles have an average diameter of 10 nm. The fringes, spaced 2.49 Å apart, can be observed clearly. These are assigned to the (111) planes of β-SiC. The value is close to the literature data for β-SiC, 0.252 nm.[15] In addition, **II** is confirmed to be β-SiC, based on the results from XRD, FTIR, Raman, and XPS studies. It is interesting to note that, as suggested by a qualitative comparison of the XPS results, **II** contained less free carbon than did **I**; this may rationalize the apparent color difference between **I** and **II**, which are black and yellow, respectively.

We studied how the physical shapes of **I** and **II** were influenced by the precursors **Pre-I** and **Pre-II**. Formed at 623 K, **Pre-I** showed cubic structures upon examination by SEM. EDS and XRD studies indicated the presence of NaCl, a by-product in the reaction. The TGA result showed that **Pre-I** contained a material that decomposed significantly above 873 K. FTIR and ^{29}Si SSNMR data supported the hypothesis that **Pre-I** was a polycarbosilane.[16] According to the original Yajima studies, the polycarbosilane was formed from a linear poly(dimethylsilane), which was the initial product generated from the coupling of $SiMe_2Cl_2$ by Na.[10] Based on the above information, we suggest that **Pre-I** had cubic cores of NaCl crystals, which served as self-generated templates that supported flexible shells composed of the linear polycarbosilane. At 1273 K under vacuum, the inner cores were vaporized while the outer shells were decomposed into **I**, the cubic cages and shells of β-SiC. The overall reaction steps to the products are summarized in Figure 3. For **Pre-II**, the presence of NaCl and polycarbosilane was also supported by XRD, FTIR, and ^{29}Si SSNMR data. However, since **II** were nanoparticles displaying a physical shape distinctively different from **I**, we speculate that **Pre-II** did not have a tightly attached NaCl/polycarbosilane core–shell structure similar to that observed for **Pre-I**. Instead, the polymer and the salt might grow into widely separated phases with little structural correlation. Based on a previous report,[17] the initial coupling product between $SiMeCl_3$ and Na at 623 K is proposed to be polymethylsilyne, $(MeSi)_n$, a highly crosslinked polymer network. This material might further react to form rigid, crosslinked polycarbosilane-based nanoparticles of **Pre-II**. This is supported by the TGA result that **Pre-II** was thermally much more stable than **Pre-I**. Then, at 1273 K, these nanoparticles were converted into β-SiC **II**.

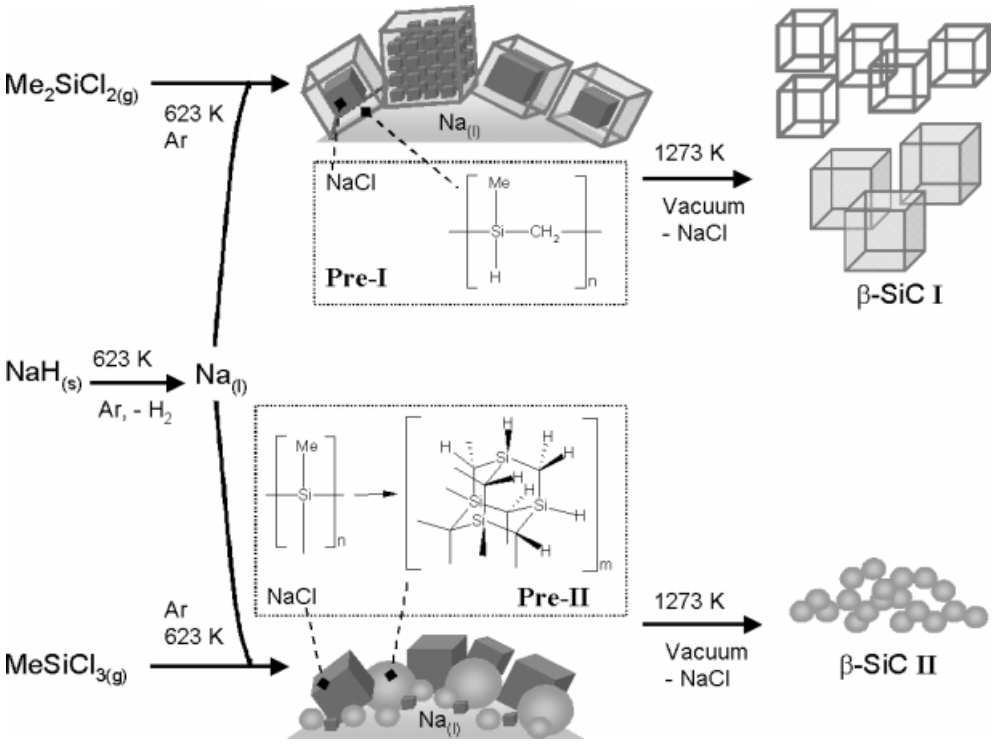

Figure 3. Reaction scheme for formation of **I** and **II**.

In conclusion, we have synthesized β-SiC cages, cubes, and nanoparticles via vapor–liquid reactions employing methylchlorosilanes and Na. The route is a simplified solvent-free Yajima process. This interesting example shows how non-volatile products produced at the vapor–liquid interface may cooperatively influence the physical appearance of the final product. Both the precursors **Pre-I** and **Pre-II** were composed of mixtures of polycarbosilane and NaCl. In **Pre-I**, the flexible, linear polycarbosilane was probably wrapped around the NaCl crystals completely, which served as cubic templates. The cubic shape was maintained in the final product **I**. By contrast, in **Pre-II**, the rigid, crosslinked polycarbosilane separated completely from the NaCl crystals. This resulted in the observation of little structural influence and correlation, and the final product, **II**, formed as featureless nanoparticles. The differences between the precursors generated pronounced shape variations in the final products of β-SiC. Clearly, the difference in appearance between **I** and **II** is the consequence of the difference in interaction between the phase-separated solid products generated at the interface of the vapor–liquid/solid reactions. This type of behavior has been observed in other systems.[18,19] Search for potential applications of these new materials is in progress.

Experimental

In a typical reaction, NaH powder (Aldrich, 0.20 g, 8.3 mmole) in a quartz boat was placed in a 30 mm quartz tube and heated in a horizontal-tube furnace at 623 K under 1 atm of pressure (1 atm = 101.325 kPa) and Ar flow (flow rate: 20 sccm) for 1 h. At 1 atm and 255 K, a methylchlorosilane, either $SiMe_2Cl_2$ or $SiMeCl_3$, was evaporated into the reactor. The reaction was carried out at 623 K under the assistance of a constant flow of Ar (1–2 sccm) for 20 h to generate a precursor. **Pre-I** and **Pre-II** were formed from $SiMe_2Cl_2$ and $SiMeCl_3$, respectively. Then, the precursor was calcined at 1273 K for 1 h under vacuum. From **Pre-I**, a black powder, **I**, was obtained. From **Pre-II**, a yellow powder, **II**, was isolated.

Scanning electron microscopy and energy dispersive spectroscopy data were collected using Hitachi S-4000 and JEOL JSM-6330F instruments at 15 kV. Transmission electron microscopy (TEM) and electron diffraction images were obtained on Philips TECNAI 20 and JEOL JEM-2010 instruments at 200 kV. High-resolution TEM images were acquired on a JEOL JEM-4000EX at 400 kV. X-ray diffraction studies were carried out using MAC MXP-18 and Bruker AXS D8 Advance diffractometers with Cu $K\alpha_1$ radiation. Fourier-transform IR spectra were collected using a Nicolet Avatar 360. Raman spectra of the samples were measured using a Jobin Yvon T-64000 equipped with an Ar^+ laser (514.5 nm, 30 mW) and a triple monochromator. X-ray photoelectron spectroscopy measurements were carried out using a Perkin–Elmer PHI-1600 spectrometer with Mg Kα (1253.6 eV) radiation. Thermal gravimetric analysis (TGA) data were collected using a Seiko SSC 5200 TGA under Ar.

Received: June 12, 2004
Final version: October 17, 2004

[1] D. K. Ferry, *Phys. Rev. B: Solid State* **1975**, *12*, 2361.
[2] T. Sakka, D. D. Bidinger, I. A. Aksay, *J. Am. Ceram. Soc.* **1995**, *78*, 479.
[3] N. Kilinger, E. Strauss, K. L. Komareh, *J. Am. Ceram. Soc.* **1966**, *49*, 369.
[4] J. J. Biernacki, G. P. Wotzak, *J. Am. Ceram. Soc.* **1989**, *72*, 122.

ADVANCED MATERIALS

[5] F. Hatakeyama, S. Kanzaki, *J. Am. Ceram. Soc.* **1990**, *73*, 2107.
[6] I. S. Seog, C. H. Kim, *J. Mater. Sci.* **1993**, *28*, 3227.
[7] Y. Kamlag, A. Goossens, I. Colbeck, J. Schoonman, *Chem. Vap. Deposition* **2003**, *9*, 125.
[8] H.-T. Chiu, S.-C. Huang, *J. Mater. Sci. Lett.* **1993**, *12*, 537.
[9] M. W. Pitcher, S. J. Joray, P. A. Bianconi, *Adv. Mater.* **2004**, *16*, 706.
[10] S. Yajima, J. Hayasht, M. Omori, *Chem. Lett.* **1975**, 931.
[11] S. Yajima, K. Okamura, J. Hayasht, *Chem. Lett.* **1975**, 1209.
[12] S. Yajima, M. Omori, J. Hayasht, K. Okamura, *Chem. Lett.* **1976**, 551.
[13] S. Yajima, J. Hayasht, Y. Hasegawa, M. Iimura, *J. Mater. Sci.* **1978**, *13*, 2569.
[14] S. Yajima, Y. Hasegawa, M. Omori, K. Okamura, *Nature* **1976**, *261*, 683.
[15] Joint Committee on Powder Diffraction Standards (JCPDS) File No. 29–1129, International Center for Diffraction Data, **1982**.
[16] T. Iseki, M. Narisawa, Y. Katase, K. Oka, T. Dohmaru, K. Okamura, *Chem. Mater.* **2001**, *13*, 4163.
[17] P. A. Bianconi, T. W. Weidman, *J. Am. Chem. Soc.* **1988**, *110*, 2342.
[18] M.-Y. Yen, C.-W. Chiu, C.-H. Shia, F.-R. Chen, J.-J. Kai, C.-Y. Lee, H.-T. Chiu, *Adv. Mater.* **2003**, *15*, 235.
[19] C.-H. Hsia, M.-Y. Yen, C.-C. Lin, H.-T. Chiu, C.-Y. Lee, *J. Am. Chem. Soc.* **2003**, *125*, 9940.

Back-Side Electrical Contacts for Patterned Electrochromic Devices on Porous Substrates**

By *Avni A. Argun*, *Mathieu Berard*, *Pierre-Henri Aubert*, and *John R. Reynolds**

Patterning of electrodes for electronic devices is essential for fabrication of fine-structured circuits, independently addressed display devices with high resolution, and devices which require separation of adjacent electrodes. Conventional direct-writing methods, such as photolithography, are widely used due to their nanometer-scale resolution, but suffer from multi-step preparation procedures and high cost. Soft-lithography techniques such as microcontact printing (μCP)[1] employ molds and masks, and have proven useful since they are non-reactive and require milder processing conditions. Other methods include, but are not limited to, metal-vapor deposition through shadow masks, line patterning,[2] screen printing,[3] and inkjet printing.[4] Electrical contact to electromagnetically active devices, such as integrated electronics, electroluminescent, photovoltaic, electrochromic, and other devices, is typically provided using electrically conductive traces which connect electrodes to conductive structures disposed on the same side of a device. The conductive traces and bond pads can significantly diminish the available surface area for active devices. Moreover, such arrangements can introduce performance limitations, as well as affect the appearance of the device for display applications, such as for certain electrochromic- and electroluminescent-display devices. As an example, our group has recently developed multipixel, dual-colored polymer electrochromic devices (ECDs) based on gold-coated porous electrodes.[5] Porous membranes were patterned by evaporation of gold through a shadow mask under high vacuum, which enabled electropolymerization and independent electrochromic switching of at least two different electrochromic polymers on these laterally configured pixels. These devices then can display a set of colors on a device to create high-contrast surfaces. Appearance of electrical-contact traces between these independently addressed pixels revealed the need for a technique to bring the pixels closer together (making the traces invisible) without compromising conductivity or performance.

[*] Prof. J. R. Reynolds, Dr. A. A. Argun, M. Berard, Dr. P.-H. Aubert
The George and Josephine Butler Polymer Research Laboratory
Department of Chemistry
Center for Macromolecular Sciences and Engineering
University of Florida
Gainesville, FL 32611 (USA)
E-mail: reynolds@chem.ufl.edu

[**] We gratefully acknowledge funding from the AFOSR (F49620–03–1–0091) and the ARO/MURI (DAAD19–99–1–0316). Supporting Information is available online from Wiley InterScience or from the author.

  DOI: 10.1002/adma.200401353